Available online at www.sciencedirect.com
SCIENCE DIRECT®
Journal of the European Ceramic Society 25 (2005) 3579–3585
www.elsevier.com/locate/jeurceramsoc

Densification of nanocrystalline MgO ceramics by hot-pressing

David Ehre, Elazar Y. Gutmanas, Rachman Chaim*

Department of Materials Engineering, Technion—Israel Institute of Technology, Haifa 32000, Israel

Received 8 June 2004; received in revised form 13 September 2004; accepted 18 September 2004
Available online 7 December 2004

Abstract

Densification of pure nanocrystalline MgO powder with 10 nm particle size by hot-pressing was investigated in the temperature range 700–800 °C, applied pressure range 100–200 MPa, and for durations of up to 240 min. It was shown that significant densification under the pressure begins above 440 °C. Densities higher than 99.5% with grain size of 73 nm were achieved at 790 °C and 150 MPa for a 30 min duration. Remarkable densification from 90 to 99.5% was observed by temperature change from 700 to 790 °C, for which the grain size was doubled only. The final grain size decreased with increasing the applied pressure. Higher shrinkage rates and cumulative shrinkages were recorded by the application of pressure at 550 °C rather than from room temperature. The temperature at which the pressure was applied is crucial in determining the maximum shrinkage rate in the nanocrystalline compacts. This effect was related to the morphological changes of the particles caused by plastic deformation at lower temperatures. Analysis of the densification rate and its comparison to the literature data was in agreement with Coble creep, where self-diffusion of Mg^{2+} cations along the grain boundaries acts as a main densification mechanism.

Keywords: Nanocrystalline; Densification; Hot-pressing; MgO

1. Introduction

Effects of the nanocrystalline character on the various properties of structural and functional ceramics become important with miniaturization of devices and technological systems. For exploring such effects, dense nanocrystalline ceramics are needed as model systems. Fabrication of dense bulk nanocrystalline oxides is very challenging since inevitable grain growth occurs at relatively high sintering temperatures needed for densification. MgO has high melting temperature (~2850 °C) and temperatures as high as 1700 °C were reported for pressureless sintering of micron size MgO powder to full density.[1–3] This has motivated fabrication of the nanocrystalline MgO (nc-MgO) powders formed from hydroxide precursor prior to compaction.[4–6] Decrease in the particle size of the MgO powder into the nanometer range (11–260 nm) resulted in nearly fully dense specimens with sub-micron grain size.[4] Hot-pressing was used in order to decrease the densification temperature and resulted in a finer grain size.[7–12] Pressure calcintering of magnesium hydroxide powders resulted in fully dense MgO at 1000 °C under the pressure of 46 MPa albeit with micrometer size grains.[7] Translucent specimens were obtained by hot-pressing at 1100 °C for 1 h.[12] Recently, translucent MgO ceramics were also fabricated by hot-pressing of nanopowders.[13] However, the average grain size in these MgO ceramics was above a few micrometers, most probably due to high hot-pressing temperatures above 1000 °C.

The present paper describes methodological hot-pressing experiments through which effects of the pressure, temperature, and duration as well as pressure application regime for full densification of nc-MgO was investigated. It is shown that temperatures between 700 and 800 °C suffice for full densification of nc-MgO.

2. Experimental procedures

Highly pure nc-MgO powder (Nanomaterials Res. Inc.) formed by chemical precipitation with specific surface area of 145 m^2/g and calculated spherical diameter of 11 nm was

* Corresponding author. Tel.: +972 4 8294589; fax: +972 4 8321978.

0955-2219/$ – see front matter © 2004 Elsevier Ltd. All rights reserved.
doi:10.1016/j.jeurceramsoc.2004.09.023

used. The impurity content was (in ppm): 100 Fe, 76 Na, 70 Al, 30 Sn, 25 As, 14 Mn, 10 Bi, 10 Pb, 8 Ca, and 7 K. The as-received powder was uniaxially cold pressed at 30 MPa into cylindrical compacts, 15 mm in diameter and 15 mm height and the relative density up to 30%. The ash-free lubricant was used for die wall lubrication. This was followed by cold isostatic pressing (CIP) at 250 MPa, where the green density increased up to 51%. In order to prevent moisture absorption, the green compacts were kept within a desiccator evacuated to 0.8 mbar, until the hot-pressing step. The hot-pressing experiments were performed in air at the temperature range 700–800 °C, the pressure range 100–200 MPa, and duration up to 4 h. Instron 8500 testing machine with boron-nitride coated Inconel dies placed into cylindrical furnace was used. The external surfaces of the hot-pressed samples were ground to remove surface layers that may be affected by the lubricating BN coating. The pressure was applied either at room temperature or at higher temperatures as indicated.

The powder shrinkage behavior was characterized using dilatometer (Linses-75) at the heating rate of 5 °C/min. The linear shrinkage of the disc thickness was measured during the hot-pressing. Since the mass and diameter were constant during the hot-pressing, this linear shrinkage represents fairly well the volume shrinkage. The final density of the specimens was measured by the Archimedes technique using the 2-propanol as the immersion liquid. The microstructure of the powder and the dense specimens were characterized using transmission electron microscopy (TEM, JEOL 2000FX, operated at 200 kV) and high resolution scanning electron microscopy (HRSEM, Leo Gemini 982 FEG operated at 4 kV). The specimens were not coated for the TEM/HRSEM observations.

HRSEM images were used for image analysis (Scion image-NIH) to determine the median grain size as well as the grain size distribution, where 200 grains were counted at least for a given specimen statistics.

3. Results

The as-received powder exhibited polyhedral shape crystallites with average diameter of ∼10 nm arranged in porous agglomerates (Fig. 1). In order to determine the powder shrinkage behavior and the optimal densification temperature range, the linear shrinkage of a 5 mm in diameter and 10 mm long CIPed nc-MgO rod was recorded in dilatometer (Fig. 2). The shrinkage began already at 100 °C and increased continuously with temperature; the main shrinkage started at 700 °C and continued up to 1600 °C. The 2% shrinkage between 100 and 400 °C is related to the burnout of the excess lubricant and was neglected. The additional linear shrinkage was ∼21% which is comparable to ∼63% volumetric shrinkage, assuming homogeneous and isotropic shrinkage. The maximum shrinkage rate at the inflection point of this curve was at ∼1180 °C. The coefficient of the linear thermal expansion (CTE) derived from the slope of the cooling curve

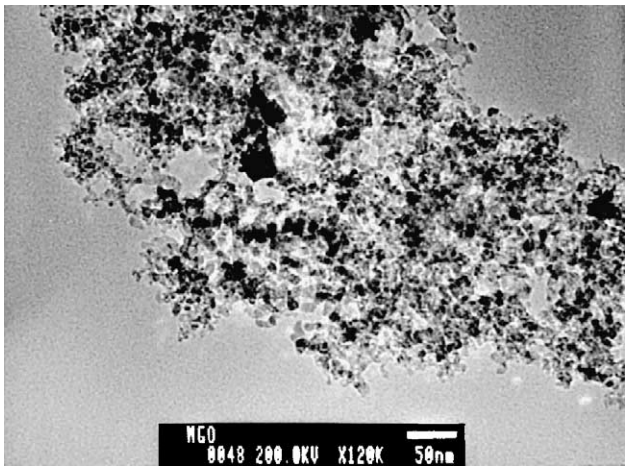

Fig. 1. TEM image of the nc-MgO powder exhibiting agglomeration of 10 nm equiaxed polyhedral shape crystallites. The scale bar is 50 nm.

was $10.2 \times 10^{-6}\,°C^{-1}$ compared to $13.5 \times 10^{-6}\,°C^{-1}$, the mean CTE for conventional MgO.[14]

The effect of the applied pressure on the volume shrinkage versus temperature was investigated in Instron machine (8500) at 50 and 150 MPa, as shown in Fig. 3a. Since the diameter of the compact is considered to be constant during the hot-pressing due to the die diameter constraint, the measured linear shrinkage is referred as the volume shrinkage of the compact. No shrinkage was observed below 400 °C at 50 MPa pressure. The shrinkage curve at this lower pressure exhibited a sigmoidal character similar to that expected from the load-free shrinkage curve (Fig. 2) though the onset temperature for shrinkage start was shifted to lower temperatures. For comparison, continuous shrinkage was observed already from room temperature at 150 MPa (Fig. 3a). Since the heating rate was constant, the slopes of the two curves in Fig. 3a are directly proportional to their densification rates. At higher pressure of 150 MPa the shrinkage curve may be approximated by two linear lines, the latter above ∼440 °C exhibiting much higher shrinkage rate than the former below

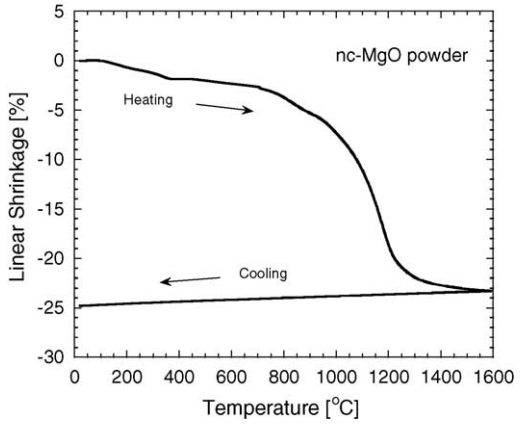

Fig. 2. Dilatometric linear shrinkage curve of the cold isostatically pressed nc-MgO compact vs. temperature.

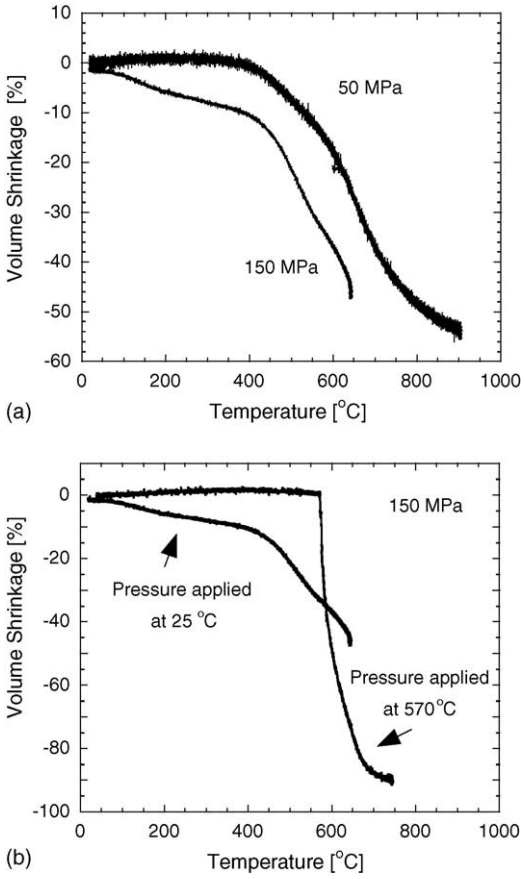

Fig. 3. (a) Effect of the applied pressure and (b) of the pressure application regime on volume shrinkage during hot-pressing of nc-MgO compacts. Application of pressure at 570 °C significantly increased the densification rate.

this temperature. The reason for this change in the densification rate was further explored and will be discussed below. Therefore, effective densification of the green nc-MgO compact necessitates application of the critical temperature and pressure.

The effect of the regime at which the pressure may be applied on the volume shrinkage was studied using 51% dense CIPed compacts. Application of a constant pressure (150 MPa) already at room temperature has led to cumulative volume shrinkage of 45% at 640 °C as shown in Fig. 3b. On the other hand, when the same pressure was applied but only at 570 °C, a much higher shrinkage rate was observed resulting in cumulative volume shrinkage of 75% at 640 °C and 88% at 700 °C. It appears that the temperature at which the pressure is applied is crucial for determining the maximum shrinkage rate in these nanocrystalline compacts.

The volume shrinkage versus temperature (up to 720 °C) at three different pressures applied at 550 °C is shown in Fig. 4. Generally, the observed densification rates were very fast and similar to one another, immediately after the pressure application and at shrinkage values below 20%. The cumulative volume shrinkage increased at higher temperatures with increase in the applied pressure, however, by a few (i.e. 2 to 8)

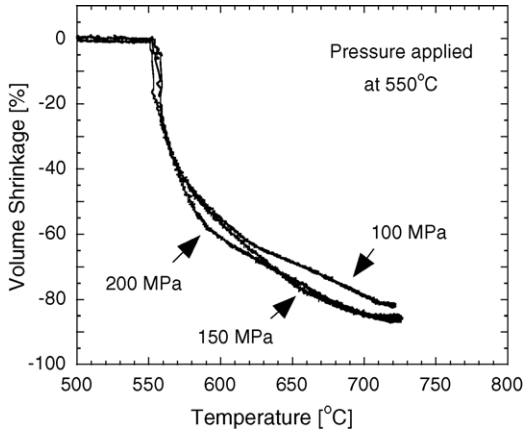

Fig. 4. Effect of applied pressure on volume shrinkage vs. temperature.

percents. At this stage, the relative densities ranged between 93 and 95%.

The volume shrinkage versus time under the applied pressure of 200 MPa is shown in Fig. 5 together with the heating curve. It was apparent that significant densification occurred immediately after the pressure application at 550 °C. The maximal shrinkage of 85% was reached within 15 min from the pressure application. The volume shrinkage curve reached a saturation level before the actual hot-pressing temperature (720 °C) was reached. At this stage, the relative density of the specimen is about 92%. In order to follow the effect of the hot-pressing temperature on the overall shrinkage behavior, the hot-pressing temperature was changed within the 720–790 °C range, while 150 MPa pressure was applied starting at 550 °C (Fig. 6). Very rapid and comparable shrinkage rates (slope of the curves) were observed for the first 20% shrinkage, regardless of the maximal hot-pressing temperature. However, the shrinkage rate beyond 20% was found to monotonically decrease to zero. At these shrinkage values, faster shrinkage rates were associated with higher hot-pressing temperatures. The cumulative volume shrinkages near saturation varied only by a few percents for different temperatures.

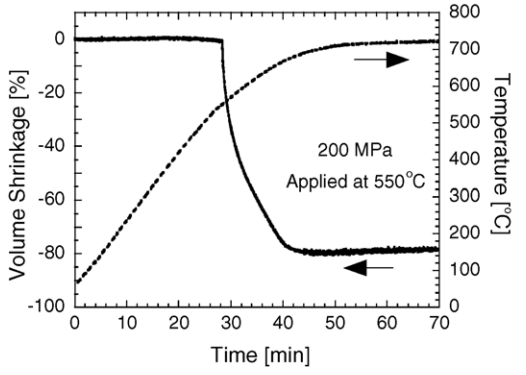

Fig. 5. Volume shrinkage vs. heating time for hot-pressing at 720 °C. The pressure was applied at 550 °C. The maximum shrinkage is reached within 15 min already during the heating.

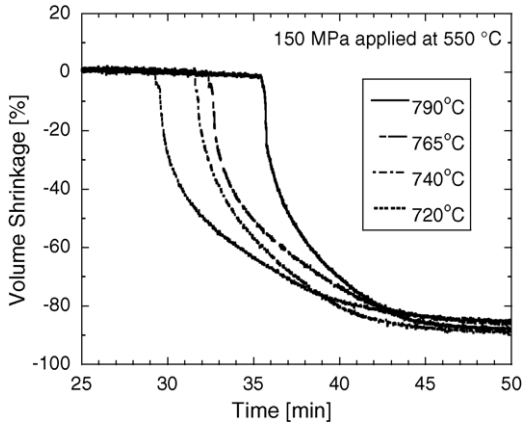

Fig. 6. Volume shrinkage vs. heating time for hot-pressing at 720 °C. The pressure was applied starting at 550 °C. The maximum shrinkage is reached within 15 min already during the heating.

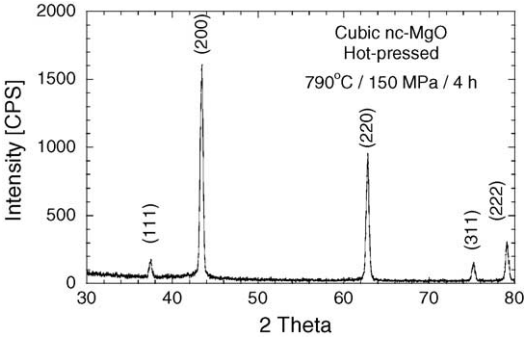

Fig. 7. X-ray diffraction from the hot-pressed nc-MgO.

X-ray diffraction spectrum from the hot-pressed nc-MgO specimens revealed their rock-salt cubic crystal structure (i.e. Fig. 7). Typical HRSEM images taken from the nc-MgO hot-pressed at different pressures are shown in Fig. 8. Although these dense specimens exhibited nano-size grains, image analysis of such micrographs revealed the wide grain size distribution with log-normal character (Fig. 9). The main microstructural feature of these dense specimens was the polyhedral shape of the hot-pressed grains that resembled the original polyhedral shape of the powder particles. The

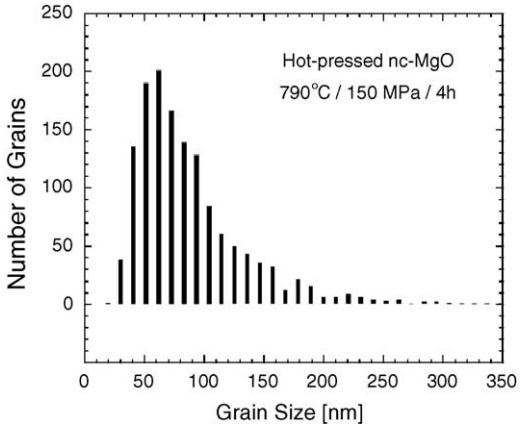

Fig. 9. The log-normal grain size distribution in the hot-pressed nc-MgO.

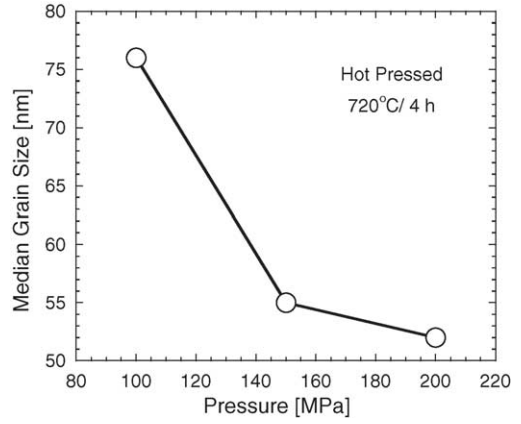

Fig. 10. Effect of the applied pressure on the mean grain size resulting from hot-pressing of nc-MgO for 4 h at 720 °C.

size of the regions suspected as pore was of the same order or lower than the grain size. In this respect, the effect of pressure on the grain size at 720 °C for 4 h hot-pressing duration is shown in Fig. 10. The density at these conditions ranged between 92 and 95%. The effect of pressure on grain growth inhibition was clearly observed. The median grain size was 76 nm under the 100 MPa pressure compared to 52 nm under 200 MPa.

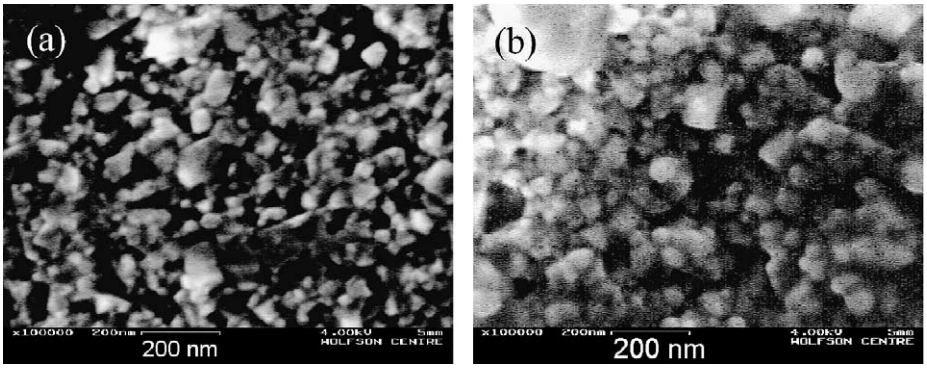

Fig. 8. HRSEM of the nc-MgO hot-pressed for 4 h at 720 °C and different pressures. (a) 200 MPa with average grain size of 52 ± 27 nm. (b) 100 MPa with average grain size of 76 ± 35 nm. The scale bar is 200 nm.

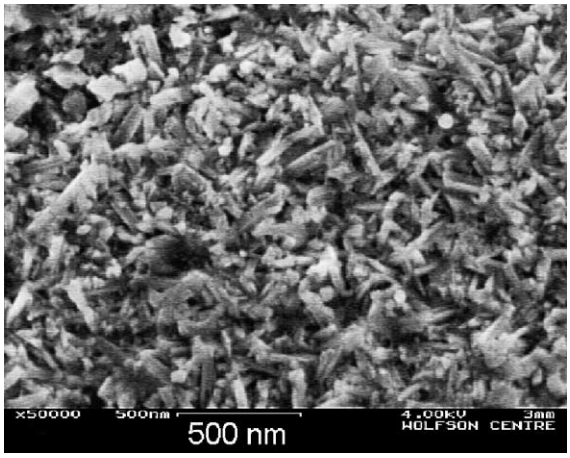

Fig. 11. HRSEM image from the fracture surface of nc-MgO hot-pressed at 150 MPa up to 650 °C and air cooled. The acicular and distorted nano-grains indicate fragmentation during the low temperature densification. The scale bar is 500 nm.

In order to explore the cause for the change in the densification rate with temperature (Fig. 3) one specimen was pressed at 150 MPa already from room temperature up to 650 °C, followed by pressure release and rapid cooling to room temperature. The fracture surface of this specimen that was examined in HRSEM, exhibited elongated grains (Fig. 11) which resemble a microstructure typical of plastically deformed grains within partially dense compact. The origin of this microstructure will be discussed below.

The overall results indicated that significant densification under the pressure may begin above 440 °C. Nevertheless, pressureless densification within dilatometer (Fig. 2) and temperature–pressure densification pattern (Fig. 3) revealed that significant shrinkage started only above 550 °C. Since grain growth is expected to occur around 900 °C,[1,4] the hot-pressing temperature window was set between 700 and 800 °C. The overall density–grain size–hot-pressing temperature pattern for 4 h duration under 150 MPa pressure applied at 550 °C is presented in Fig. 12. The relative density was 90% at 700 °C and increased to more than 99.5% at 790 °C. Then, the corresponding grain sizes changed from 43 to 73 nm, respectively. Such changes in the grain size are considered to be small compared to the accelerated grain growth that is expected in compacts with relative densities above 90%. The present results clearly show that fully dense nanocrystalline MgO can be fabricated by application of appropriate hot-pressing conditions at elevated temperatures and for relatively short durations.

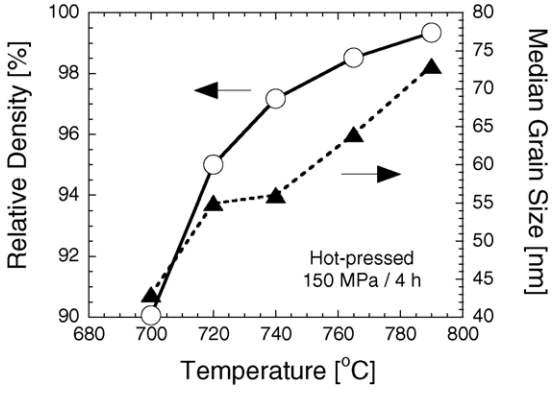

Fig. 12. Relative density and grain size of nc-MgO hot-pressed at 150 MPa and different temperatures. The grain size at the final stage of densification was only doubled.

4. Discussion

The pressure level and the temperature at which it applied are very important in determining the maximum shrinkage rate. In this respect, application of pressure from room temperature was found to lead to plastically deformed elongated grains. Two deformation processes may be considered while applying pressure on the green compact already from room temperature. First, plastic deformation of the compact by particles' sliding over each other to fill the residual pores. This process is not likely to occur at room temperature, since the present compacts were CIPed at much higher pressure of 250 MPa prior to hot-pressing. The high frictional forces between the particles may be overcome only at higher temperatures where suffice surface diffusion exists. The second process is by plastic deformation of the grains to form extrusions through the residual porosity. This process, which is aided by the frictional forces between the particles, may lead to strain hardening and fracture. Since the densification below 440 °C require a threshold stress (Fig. 3a) it may be related both to plastic deformation of nanoparticles and fragmentation of their agglomerates. This trend is very plausible at lower temperatures due to the low hardness of MgO (7 GPa)[14] and its low room temperature yield stress both in bending (138 MPa)[15] and in compression (75 to 140 MPa).[15,16] Flow of MgO under high hydrostatic pressures (up to 1000 MPa) at room temperature exhibited low work hardening rate up to 3% strain followed by steeper work hardening rate up to 15% strain, where fracture was occurred.[17] Similar strain hardening behavior with stress exponent of unity was observed under lower stress of 140 MPa between 700 and 860 °C in MgO with submicron grain size.[18] These data support the relatively large plastic strains observed in the nanocrystalline grains (Fig. 11). However, this plastic strain is limited (∼15%) due to strain hardening and can lead to limited densification at lower temperatures. On the other hand, cyclic deformation of MgO single crystals has shown that plastic recovery occurs between 400 and 470 °C, mainly by screw dislocations.[19] This strain recovery may partially explain the higher densification rate that was observed above 440 °C where the pressure was applied from room temperature (Fig. 3a). Investigation of the hot-pressing kinetics of ultrafine MgO between 500 and 700 °C and between 60 and 295 MPa, showed the Coble

creep (via grain boundary sliding) as the dominating densification mechanism.[16,20] Therefore, application of pressure at room temperature results in morphological changes of the grains (i.e. change in the grain aspect ratio). Further densification at higher temperatures by grain boundary sliding may be inhibited by interlocked grain morphology. The 150 MPa curve (Fig. 3a) exhibited densification below 440 °C compared to no densification under 50 MPa pressure; the later is apparently lower than the yield stress of the nanocrystals. However, the slopes of the two curves become comparable above 440 °C. The weaker pressure effect on the densification rate of the two curves above 440 °C may also be explained by mutual sliding of the grains over each other, once a temperature is high enough for releasing the frictional forces by surface diffusion as mentioned above. In this respect, application of pressure only at higher temperatures (i.e. 570 °C in Fig. 3b) leads to densification by sliding of equiaxed particles over each other. Therefore, higher densification rate and cumulative shrinkage is expected for sliding of equiaxed grains compared to those of elongated grains.

It was further found that significant densification begins immediately at pressure application around 550 °C (Fig. 6). Nevertheless, densification tends to saturate within the time interval of 15 to 30 min after this rapid shrinkage. Comparing the shrinkage behavior with respect to temperature and pressure, a pronounced effect of the applied pressure on density was observed (compare Fig. 2 without pressure and Fig. 4 with pressure). This behavior may be expected in the light of the high pressures applied in comparison to the capillary forces; the later comprise the driving force for pressureless sintering. The driving force ΔP, during hot pressing of the green powder compact with average particle radius r, under the applied pressure P_{Applied}, is given by:[21]

$$\Delta P = P_{\text{Applied}} - \frac{2\gamma_{\text{SV}}}{r} \quad (1)$$

where γ_{SV} is the solid–vapor surface energy. For the particle size of 10 nm and surface energy of 0.12 J m^{-2} (see Ref. 22) the driving force for pressureless sintering (i.e. capillary forces) is about 24 MPa, which is four to eight times lower than the applied pressures (100 to 200 MPa). In addition, some coarsening of the particles during the heating to the hot-pressing temperature may further decrease the corresponding capillary forces. Therefore, the contribution of the applied pressure to densification is very high. For comparison, hot-pressing of nanocrystalline MgO with 30 nm particle size for 30 min at 500 °C and in the 6 to 28 GPa pressure range has led to final densities ranging from 41 to 90%, respectively.[9] The stress exponent during the hot-pressing at 500 °C was 1.14, very close to unity for which diffusional processes were suggested as densification mechanisms. The actual strain rates ranged between 0.021 and 0.132 s^{-1}, respectively. However, hot-pressing of MgO with submicrometer grain size (0.1 to 0.5 μm) at much higher temperatures, i.e. 1600 °C and the pressure range 5–30 MPa yielded stress exponent of 3 at constant density of 80%, which was related to dislocation creep.[11] The corresponding densification rates were between 10^{-5} and 10^{-3} s^{-1}.

Although rapid densification immediately after pressure application (Fig. 6) may be associated with particle sliding aided by surface diffusion, the last stages of densification (i.e. 80% volume shrinkage and higher) should be related to grain boundary diffusion. This arises from the loss in continuity of the internal pores. The shrinkage curves represent the engineering strain ε for which the initial length of the specimen is assumed to be constant. However, the true strain is given by natural logarithmic of $1+\varepsilon$ from which the true strain rate may be determined. The lower shrinkage rate in the last stages of densification in the temperature range 650–700 °C at 100 MPa (Fig. 4) yields true strain rate of the order 5.5×10^{-4} s^{-1}. Using the deformation-mechanism map of ultra-fine MgO at 770 °C and 10 MPa,[23] comparable strain rates of 10^{-3} and 10^{-4} s^{-1} were obtained for 50 and 100 nm grain size, respectively. In these conditions the Coble creep is a dominating deformation mechanism controlled by diffusion of Mg^{2+} cations.[23] On the other hand, decrease of the grain size in deformation mechanism maps of MgO is associated with extension of the diffusional flow field to higher stresses.[24] Since the effect of stress on the strain rate is linear for diffusional processes, the evaluation of the actual strain rate at 100 MPa (compared to 10 MPa) may vary within one order of magnitude, in agreement with our present calculated strain rates above. According to the present analysis, Coble creep is expected to take place in the present hot-pressing conditions, and will be controlled by diffusion of Mg^{2+} cations along the nc-MgO grain boundaries.

Diffusion of Mg^{2+} cations along the grain boundaries was also the dominating flow mechanism in MgO with 1 μm grain size at 800 °C and 100 MPa (i.e. normalized shear stress of 18.7×10^{-4}).[24] However, the strain rate in the latter was 5×10^{-7} s^{-1}, lower by three orders of magnitude than the present strain rates. Consequently, the high strain rates observed here may be related to the nano-size character of the grains at the hot-pressing temperature window.

Finally, remarkable effect of the hot-pressing temperature on the final density (Fig. 12) was noted in the narrow range of temperatures. Fully dense MgO with nanometer grain size may be achieved provided that critical pressure is applied above 550 °C. Nevertheless, grain growth was inevitable once the density was higher than 90%, which is associated with the transition of continuous pores to isolated pores. Yet, the grain size was only doubled in this temperature range and preserved its nanocrystalline character.

Acknowledgments

The support of the Israel Ministry of Science through the Grant No. 1090-1-00 is gratefully acknowledged.

References

1. Gupta, T. K., Sintering of MgO: densification and grain growth. *J. Mater. Sci.*, 1971, **6**, 25–32.
2. Varela, J. A. and Whittemore, O. J., Structural rearrangement during the sintering of MgO. *J. Am. Ceram. Soc.*, 1983, **66**, 77–82.
3. Handwerker, C. A., Cannon, R. M. and Coble, R. L., Final-stage sintering of MgO. In *Advances in Ceramics*, ed. W. D. Kingery. *Structure and Properties of MgO and Al_2O_3 Ceramics*, *Vol. 10*. The ACerS Pub., Ohio, 1984. pp. 619–643.
4. Itatani, K., Itoh, A., Howell, F. S., Kishioka, A. and Kinoshita, M., Densification and microstructure development during the sintering of submicrometer magnesium oxide particles prepared by a vapour-phase oxidation process. *J. Mater. Sci.*, 1993, **28**, 719–728.
5. Itatani, K., Nomura, M., Kishioka, A. and Kinoshita, M., Sinterability of various high-purity magnesium oxide powders. *J. Mater. Sci.*, 1986, **21**, 1429–1435.
6. Tsai, M. T. and Shih, H. C., Effects of powder processing on the characterization of magnesia derived from alkoxide precursors. Part II. Compaction and sintering behavior. *J. Mater. Sci.*, 1993, **28**, 4530–4535.
7. Morgan, P. E. D. and Scala, E., The formation of fully dense oxides by pressure calsintering of hydroxides. In *Sintering and Related Phenomena*, ed. G. C. Kuczynski, N. A. Hooton and C. F. Gibbon. Gordon and Beach, New York, 1965, pp. 861–894.
8. Vasilos, T. and Spriggs, R. M., Pressure sintering: mechanisms and microstructures for alumina and magnesia. *J. Am. Ceram. Soc.*, 1963, **46**, 493–496.
9. Pampuch, R., Tomaszewski, H. and Haberko, K., Hot-pressing of active magnesia. *Ceram. Int.*, 1975, **1**, 81–86.
10. Vieira, J. M. and Brook, R. J., Kinetics of hot-pressing: the semilogarithmic law. *J. Am. Ceram. Soc.*, 1984, **67**, 245–249.
11. Vieira, J. M. and Brook, R. J., Hot-pressing of high-purity magnesium oxide. *J. Am. Ceram. Soc.*, 1984, **67**, 450–454.
12. Itatani, K., Yasuda, R., Scott Howell, F. and Kishioka, A., Effect of starting particle size on hot-pressing of magnesium oxide powder prepared by vapour-phase oxidation process. *J. Mater. Sci.*, 1997, **32**, 2977–2984.
13. Fang, Y., Agrawal, D., Skandan, G. and Jain, M., Fabrication of translucent MgO ceramics using nanopowders. *Mater. Lett.*, 2004, **58**, 551–554.
14. Barsoum, M. W., *Fundamentals of Ceramics*. McGraw-Hill, New York, 1997.
15. Parker, E. R., Ductility of magnesium oxide. In *Mechanical Properties of Engineering Ceramics*, ed. W. W. Kriegel and H. Plamour. Interscience Pub., New York, 1961, pp. 65–87.
16. Pampuch, R., Mechanisms of hot-pressing of magnesium oxide powders. *Ceram. Int.*, 1979, **5**, 76–83.
17. Auten, T. A., Radcliffe, S. V. and Gordon, R. B., Flow stress of MgO single crystals compressed along [1 0 0] at high hydrostatic pressures. *J. Am. Ceram. Soc.*, 1976, **59**, 40–42.
18. Crampon, J. and Escaig, B., High temperature creep of ultrafine-grained Fe-doped MgO polycrystals. *J. Mater. Sci.*, 1978, **13**, 2619–2626.
19. Majumdar, B. S. and Burns, S. J., TEM study of the recovery process of cyclically deformed MgO single crystal. *J. Mater. Sci.*, 1987, **22**, 1157–1162.
20. Crampon, J., The creep microstructure of ultrafine-grained MgO polycrystals. *Acta Metall.*, 1980, **28**, 123–128.
21. King, T. A., *Fundamentals of Ceramic Powder Processing and Synthesis*. Academic Press, San Diego, 1996, p. 866.
22. Wachtman, J. B., *Mechanical Properties of Ceramics*. John Wiley & Sons, New York, 1996, p. 41.
23. Crampon, J. and Escaig, B., Mechanical properties of fine-grained magnesium oxide at large compressive strains. *J. Am. Ceram. Soc.*, 1980, **63**, 680–686.
24. Frost, H. J. and Ashby, M. F., *Deformation-Mechanism Maps*. Pergamon Press, Oxford, 1982, p. 84.